


ARTICLE

Identification of FAM181A and FAM181B as new interactors with the TEAD transcription factors

Fedir Bokhovchuk¹ | Yannick Mesrouze¹ | Clara Delaunay¹ |
 Typhaine Martin¹ | Frédéric Villard² | Marco Meyerhofer¹ |
 Patrizia Fontana¹ | Catherine Zimmermann¹ | Dirk Erdmann¹ |
 Pascal Furet³ | Clemens Scheufler² | Tobias Schmelzle¹ | Patrick Chène¹ 

¹Disease Area Oncology, Novartis
 Institutes for Biomedical Research, Basel,
 Switzerland

²Chemical Biology & Therapeutics,
 Novartis Institutes for Biomedical
 Research, Basel, Switzerland

³Global Discovery Chemistry, Novartis
 Institutes for Biomedical Research, Basel,
 Switzerland

Correspondence

Dr Patrick Chène, Novartis,
 Klybeckstrasse, WKL 125 13.12, CH-4002
 Basel Switzerland,
 Email: patrick_chene@yahoo.com

Abstract

The Hippo pathway is a key signaling pathway in the control of organ size and development. The most distal elements of this pathway, the TEAD transcription factors, are regulated by several proteins, such as YAP (Yes-associated protein), TAZ (transcriptional co-activator with PDZ-binding motif) and VGLL1-4 (Vestigial-like members 1-4). In this article, combining structural data and motif searches in protein databases, we identify two new TEAD interactors: FAM181A and FAM181B. Our structural data show that they bind to TEAD via an Ω -loop as YAP/TAZ do, but only FAM181B possesses the LxxLF motif (x any amino acid) found in YAP/TAZ. The affinity of different FAM181A/B fragments for TEAD is in the low micromolar range and full-length FAM181A/B proteins interact with TEAD in cells. These findings, together with a recent report showing that FAM181A/B proteins have a role in nervous system development, suggest a potential new involvement of the TEAD transcription factors in the development of this tissue.

KEYWORDS

FAM181A, FAM181B, hippo pathway, nervous system, omega loop, protein-protein interaction, TEAD, YAP

1 | INTRODUCTION

The Hippo pathway, which is well conserved in metazoans, is linked to various biological processes, such as cell growth/proliferation and tissue homeostasis/regeneration.¹ The deregulation of this pathway in cancer has attracted a lot of interest in recent years, because its study may lead to the development of new anticancer drugs.²⁻⁵ Furthermore, because of its role in the control of organ

growth and regeneration, modulators of the Hippo pathway could prove to be interesting new molecules in regenerative medicine.^{2,6,7} The TEAD (TEA/ATTS domain) transcription factors are the most distal elements of this pathway.^{8,9} These proteins, which have no transcriptional activity on their own, need to interact with different partners to modulate gene transcription. The four human TEAD proteins are regulated by YAP (Yes-associated protein), its paralog TAZ (transcriptional co-activator with PDZ-binding motif) and VGLL1-4 (vestigial-like).¹⁰⁻¹² Human cells express only one or a subset of the *TEAD* genes, suggesting that these transcription

Fedir Bokhovchuk and Yannick Mesrouze contributed equally to this work.

factors have tissue-selective functions (e.g.,¹³). For example, the autosomal dominant eye disease Sveinsson's chorioretinal atrophy is linked to a mutation of the *TEAD1* gene.¹⁴ The *YAP* and *TAZ* genes are broadly expressed.^{4,12} *VGLL1-3* shows a tissue-specific expression pattern, while *VGLL4* is more ubiquitously expressed.¹¹ The structures of TEAD in complex with YAP,^{15,16} TAZ,¹⁷ *VGLL1*¹⁸ and *VGLL4*¹⁹ reveal that these proteins bind to an overlapping region at the surface of TEAD. The TEAD-binding domains of YAP and TAZ are very similar and are made of three distinct secondary structure elements: a β -strand, an α -helix and an Ω -loop.¹⁵⁻¹⁷ The TEAD-binding domains of *VGLL1* and *VGLL4* also contain a β -strand and an α -helix, but they lack the Ω -loop, which is key for interaction between YAP/TAZ and TEAD.^{18,19} The structures of the TAZ:TEAD¹⁷ and *VGLL4*:TEAD¹⁹ complexes show that TAZ and *VGLL4* can bind to two TEAD molecules simultaneously, but this has not yet been reported for YAP or *VGLL1-3*. The four human TEAD proteins have a similar affinity for peptides mimicking the minimal TEAD-binding domain of YAP, TAZ and *VGLL1*²⁰ suggesting that these different regulators can compete with each other to gain access to TEAD. YAP/TAZ and *VGLL1-4* are currently the most studied TEAD interactors, but publications suggest that other proteins may also modulate the activity of these transcription factors. For example, the p160 coactivator proteins have been reported to potentiate transcription from a TEAD response element.²¹ This prompted us to look for new TEAD interactors. Instead of conducting broad interactome or ChIP studies combined with complex bioinformatics analyses, we used a strategy focused on our current knowledge of the structure of the YAP:TEAD complex. Since Ω -loops do not often mediate protein-protein interactions²²⁻²⁴ and because an Ω -loop is key to the formation of the YAP:TEAD complex, we decided to look for proteins that contain this specific recognition motif. To that end, we combined the current structural data on the YAP:TEAD complex and searches in protein databases with small degenerate sequences. This approach led to the identification of the FAM181A and FAM181B proteins that bind to TEAD via an Ω -loop both in biochemical assays and in cells.

2 | RESULTS

2.1 | Identification of the FAM181A and FAM181B proteins

The X-ray structures of the YAP:TEAD complex^{15,16,20,25,26} together with the data obtained from mutational studies of YAP^{27,28} allowed us to define

residues from the Ω -loop of YAP that are key for the interaction with TEAD. This information was used to search different databases with small degenerated sequences mimicking the Ω -loop region of YAP (residues 85–99, YAP^{85–99}) (Figure S1, Material and Methods). The FAM181A and FAM181B proteins were identified using this approach. These proteins are present in species from various animal classes, such as mammals, insects and fish (Appendix S1). FAM181A and FAM181B contain a putative Ω -loop (Figure 1), but FAM181B also possesses the LxxLF motif (x = any amino acid) found in the α -helix of the TEAD-binding domain of YAP (and TAZ).²⁹ Nonetheless, the number of amino acids between this motif and the Ω -loop is greater in FAM181B (50 residues) than in YAP (14 residues) (Figure 1). A survey of the literature shows that little is known about FAM181A/B, and only one publication has studied the function of these proteins.³⁰ This *in vivo* study reveals that FAM181A/B play a role in nervous system development and function. Interestingly, the authors have noticed that a short sequence present in FAM181A/B displays a high similarity with YAP. This sequence corresponds to FAM181A^{190–205} and FAM181B^{220–235}, which we identified as putative Ω -loops. The published data also show that FAM181A/B localize to the nucleus, suggesting that they could potentially interact with TEAD, but the authors did not probe this interaction. Altogether, the presence of a putative Ω -loop in FAM181A/B and their nuclear localization prompted us to determine whether they can bind to TEAD.

2.2 | Biochemical characterization of the interaction between the Ω -loop of FAM181A/B and TEAD

Since the isolated Ω -loop region of YAP (YAP^{85–99}) has a measurable affinity for TEAD ($\sim 70 \mu\text{M}$),³¹ the corresponding regions of FAM181A/B could also interact with TEAD. We noticed that Val84^{YAP} is conserved in FAM181A (Val190^{FAM181A}) and in FAM181B (Val220^{FAM181B}) (Figure 1). As this residue may have a steric shielding effect on YAP folding²⁷, it was included in the synthetic peptides mimicking YAP and FAM181A/B. The ability of YAP^{84–99}, YAP^{85–99}, FAM181A^{190–205} and FAM181B^{220–235} to inhibit the YAP:TEAD interaction was measured in a TR-FRET assay (Figure S2).³² In agreement with earlier data³¹, YAP^{85–99} inhibits the YAP:TEAD interaction with a high double-digit micromolar IC₅₀ (Table 1). The addition of Val84^{YAP} dramatically increases potency—YAP^{84–99} is 10 times more potent than YAP^{85–99} (Table 1)—revealing that this residue is important for the YAP:TEAD interaction. The potency of

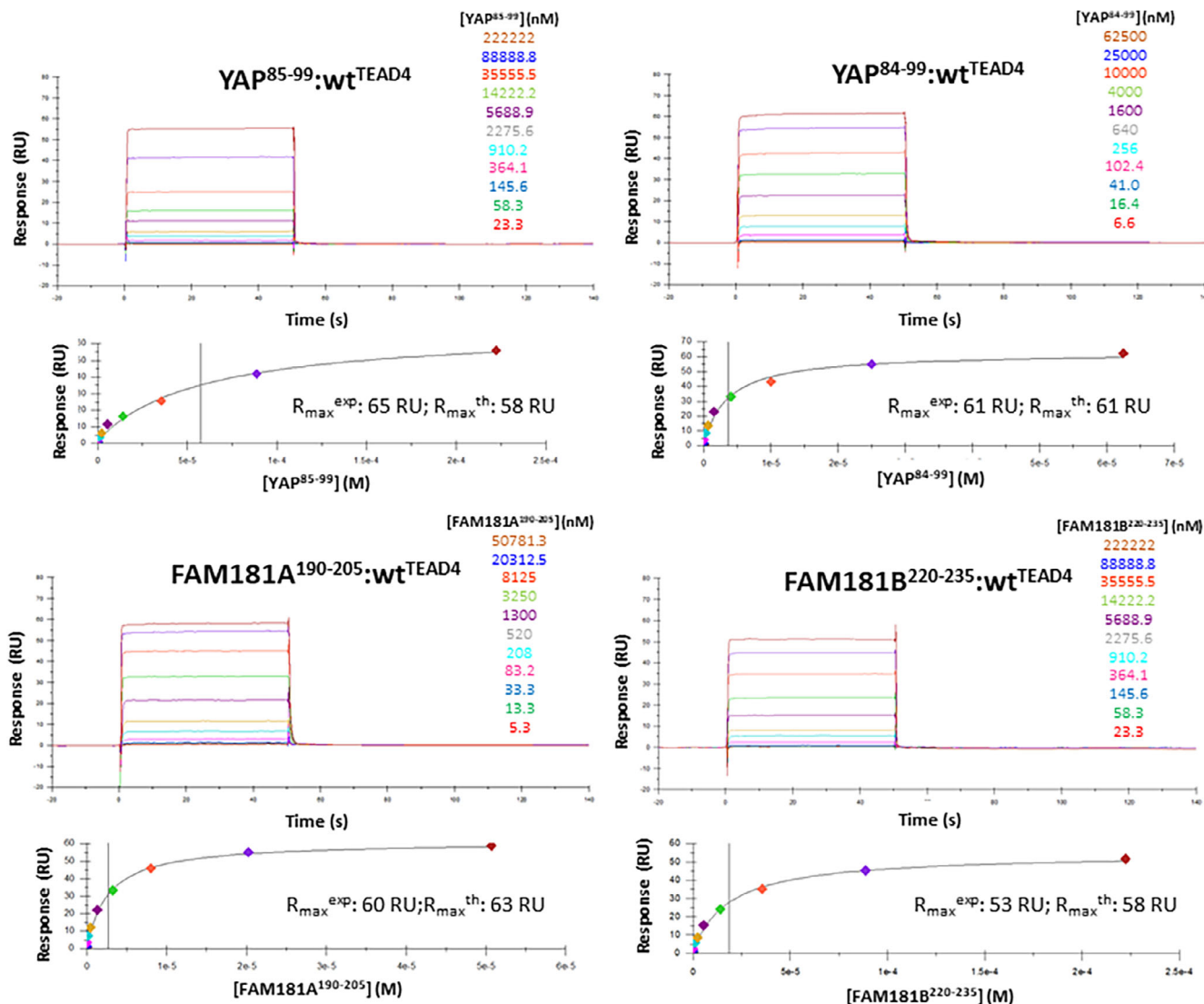


FIGURE 2 Binding of YAP⁸⁵⁻⁹⁹, YAP⁸⁴⁻⁹⁹, FAM181A¹⁹⁰⁻²⁰⁵ and FAM181B²²⁰⁻³³⁵ to TEAD4. Biotinylated N-Avitagged TEAD4²¹⁷⁻⁴³⁴ was immobilized on sensor chips, and the binding of different concentrations of YAP⁸⁵⁻⁹⁹, YAP⁸⁴⁻⁹⁹, FAM181A¹⁹⁰⁻²⁰⁵ and FAM181B²²⁰⁻³³⁵ was measured at 298 K by Surface Plasmon Resonance. The upper panels show representative sensorgrams and the lower panels the corresponding binding isotherms from which K_d values (at equilibrium) were derived. The sensorgrams were globally fitted with a 1:1 interaction model using the Biacore T200 evaluation software (Biacore, Sweden). The concentrations used are indicated. The signal measured at equilibrium (R_{\max}^{eq}) and the calculated maximum feasible signal (R_{\max}^{th}) are given

Leu227^{FAM181B} and Phe201^{FAM181A}/Phe231^{FAM181B} show hydrophobic interactions with TEAD4 similar to those of Met86^{YAP}, Leu91^{YAP} and Phe95^{YAP} (Figure 4a). These three residues also form a hydrophobic core that contributes to the stabilization of the bound Ω -loop. Trp202^{FAM181A}/Phe232^{FAM181B} are located at the top of this hydrophobic core, helping to stabilize the bound Ω -loop, and they form a cation- π interaction with Arg193^{FAM181A}/Arg223^{FAM181B} (Figure 4b). Phe96^{YAP} and Arg87^{YAP} show the same interactions in the YAP:TEAD complex (Figure 4b). The salt bridge between Arg89^{YAP} and Asp272^{TEAD4} and the hydrogen bonds between Ser94^{YAP} and Glu263^{TEAD4}:Tyr429^{TEAD4} are also present in the FAM181A/B:TEAD4 complexes.

Arg195^{FAM181A}/Arg225^{FAM181B} are in the vicinity of Asp272^{TEAD4} (Figure 4c) and Ser200^{FAM181A}/Ser230^{FAM181B} are within hydrogen bond distance from Glu263^{TEAD4}:Tyr429^{TEAD4} (Figure 4d). Pro198^{FAM181A}/Pro228^{FAM181B} hold the same position as Pro92^{YAP} at the binding interface (Figure 4d). This proline residue, which is strictly conserved in all the sequences obtained in our database search (Figure S1), is probably important for establishment of the Ω -loop conformation. Overall, the structural data confirm that FAM181A¹⁹⁰⁻²⁰⁵ and FAM181B²²⁰⁻²³⁵ form an Ω -loop upon binding to TEAD and that the key interactions of YAP with TEAD are also present in the FAM181A/B:TEAD complexes.

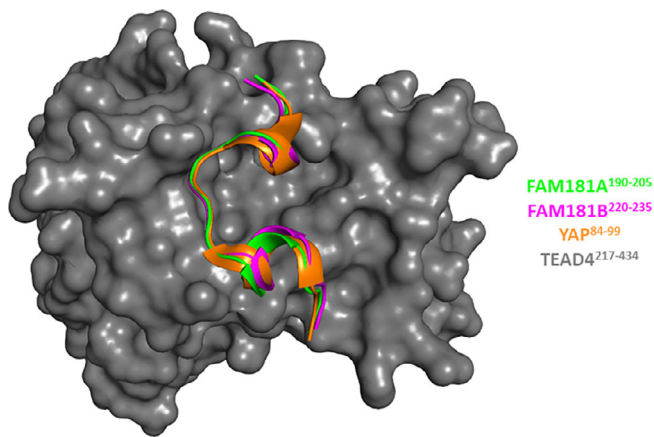


FIGURE 3 Structures of the FAM181A¹⁹⁰⁻²⁰⁵:TEAD4 and FAM181B²²⁰⁻²³⁵:TEAD4 complexes. The structures of the FAM181A¹⁹⁰⁻²⁰⁵:TEAD4 (pdb 6SEN) and FAM181B²²⁰⁻²³⁵:TEAD4 complexes (pdb 6SEO) have been superimposed on that of the YAP⁶⁰⁻¹⁰⁰:TEAD4 complex (pdb 6GE3²⁶). FAM181A¹⁹⁰⁻²⁰⁵, FAM181B²²⁰⁻²³⁵ and YAP⁸⁴⁻¹⁰⁰ are represented by green, magenta and orange ribbons, respectively. TEAD4 surface is colored gray. The picture was drawn with PyMOL (Schrodinger Inc., Cambridge, Massachusetts)

2.4 | Study of longer FAM181A/B fragments

FAM181B and YAP contain an LxxLF motif (x = any amino acid) located N-terminally of the Ω -loop (Figure 1b). In the YAP:TEAD complex, these three conserved residues make hydrophobic interactions in the α -helix binding pocket of TEAD.^{15,16} To determine the involvement of this motif (FAM181B¹⁶⁵⁻¹⁶⁹) in the FAM181B:TEAD interaction, we purified FAM181B¹⁵⁷⁻²³⁷ (Figure S3), which contains the LxxLF motif and the Ω -loop (Figure 1b). The TR-FRET and SPR results show that FAM181B¹⁵⁷⁻²³⁷ has a higher affinity for TEAD than FAM181B²²⁰⁻²³⁵ (Table 1, Figures S2 and S4). However, the potency gain is relatively small, fourfold, compared with the 84-fold gain observed with YAP [YAP⁶¹⁻⁹⁹, which contains the LxxLF motif (YAP⁶⁵⁻⁶⁹) has a $K_d = 44 \text{ nM}$ ³¹]. We next studied whether the LxxLF motif of FAM181B binds to TEAD at the same place as YAP. Val389^{TEAD4} is located in the α -helix binding pocket of TEAD and it shows van der Waals interactions with Phe69^{YAP} from the LxxLF motif. The Val389Ala^{TEAD4} mutation destabilizes the YAP:TEAD complex by 1.7 kcal/mol ($\Delta\Delta G = \Delta G^{\text{mut}} - \Delta G^{\text{wt}}$).²⁸ The K_d of FAM181B¹⁵⁷⁻²³⁷ for Val389Ala^{TEAD4} is $36 \pm 2 \mu\text{M}$ (Figure S4), showing that the mutation reduces binding by 0.94 kcal/mol. We also investigated whether this mutation affects the binding of FAM181A, which lacks an LxxLF motif. The FAM181A¹²⁷⁻²⁰⁵ construct, in which

the number of residues at the N-terminus of the Ω -loop is similar to that of FAM181B¹⁵⁷⁻²³⁷, was purified (Figure 1b and Figure S3). FAM181A¹²⁷⁻²⁰⁵ has an apparent K_d of $9.8 \pm 0.3 \mu\text{M}$ for wt^{TEAD4} (an accurate K_d could not be determined because FAM181A¹²⁷⁻²⁰⁵ binds non-specifically to sensor chips at high concentrations) and of $14.7 \pm 0.1 \mu\text{M}$ for Val419Ala^{TEAD4} (Table 1, Figure S4). Therefore, the Val419Ala^{TEAD4} mutation has little effect ($\Delta\Delta G \sim 0.2 \text{ kcal/mol}$) on the FAM181A:TEAD interaction. This suggests that FAM181A¹²⁷⁻²⁰⁵, which has no LxxLF motif, does not come into contact with Val419^{TEAD4}. The FAM181A¹²⁷⁻¹⁸⁹ region may not interact with TEAD and, if it remains in solution, this long (63 amino acids) and probably flexible fragment might destabilize the bound Ω -loop, decreasing its affinity for TEAD as observed in our experiments (FAM181A¹²⁷⁻²⁰⁵ $\text{IC}_{50}/K_d > \text{FAM181A}^{190-205}$ IC_{50}/K_d ; Table 1). To further confirm that the LxxLF motif from FAM181B interacts with TEAD4 in a manner similar to that of the corresponding motif from YAP, we conducted molecular dynamics simulations. An initial model of TEAD4²¹⁷⁻⁴³⁴ in complex with FAM181B¹⁵⁴⁻²³⁶ was constructed using the FAM181B²²⁰⁻²³⁵:TEAD4²¹⁷⁻⁴³⁴ crystal structure (pdb 6SEO) and by homology to YAP¹⁶ the N-terminal region of FAM181B¹⁵⁴⁻²³⁶ was modeled as a β -strand (FAM181B¹⁵⁴⁻¹⁵⁹) and an α -helix (FAM181B¹⁶⁰⁻¹⁷²). In this initial model, an arbitrary conformation allowing the α -helix and Ω -loop sequences to be connected in 3D was given to the linker region (FAM181B¹⁷³⁻²¹⁹). Starting from this initial model, a molecular dynamics simulation of 10 ns with an explicit water solvation model was run using the Desmond module (default parameters) in the molecular modeling package Maestro (Schrodinger Inc., Cambridge, Massachusetts). The final conformation obtained after this simulation shows that Phe169^{FAM181B} from the LxxLF motif is in the vicinity of Val389^{TEAD4} and that it occupies the same position at the binding interface as the corresponding residue from YAP, Phe69^{YAP} Figure 5. This result is in agreement with the experimental data obtained with the Val389Ala^{TEAD4} mutant. The simulation also gives an idea of the dynamics of the linker region. The β -strand: α -helix and the Ω -loop regions of FAM181B¹⁵⁴⁻²³⁶ were quite stable during the simulation (Figure S5). Only small fluctuations of some residue side chains were observed, while the main chains retained their secondary structures. However, the linker region (FAM181B¹⁷³⁻²¹⁹) showed substantial flexibility with no observable regular secondary structure and a tendency to fold back on the α -helix region towards the end of the simulation (Figure S5). This shows that, once bound to TEAD, FAM181B¹⁵⁴⁻²³⁶ remains quite flexible because of the presence of a long linker between its α -helix and its Ω -loop.

We next studied the structure of unbound FAM181A¹²⁷⁻²⁰⁵ and FAM181B¹⁵⁷⁻²³⁷ by circular dichroism

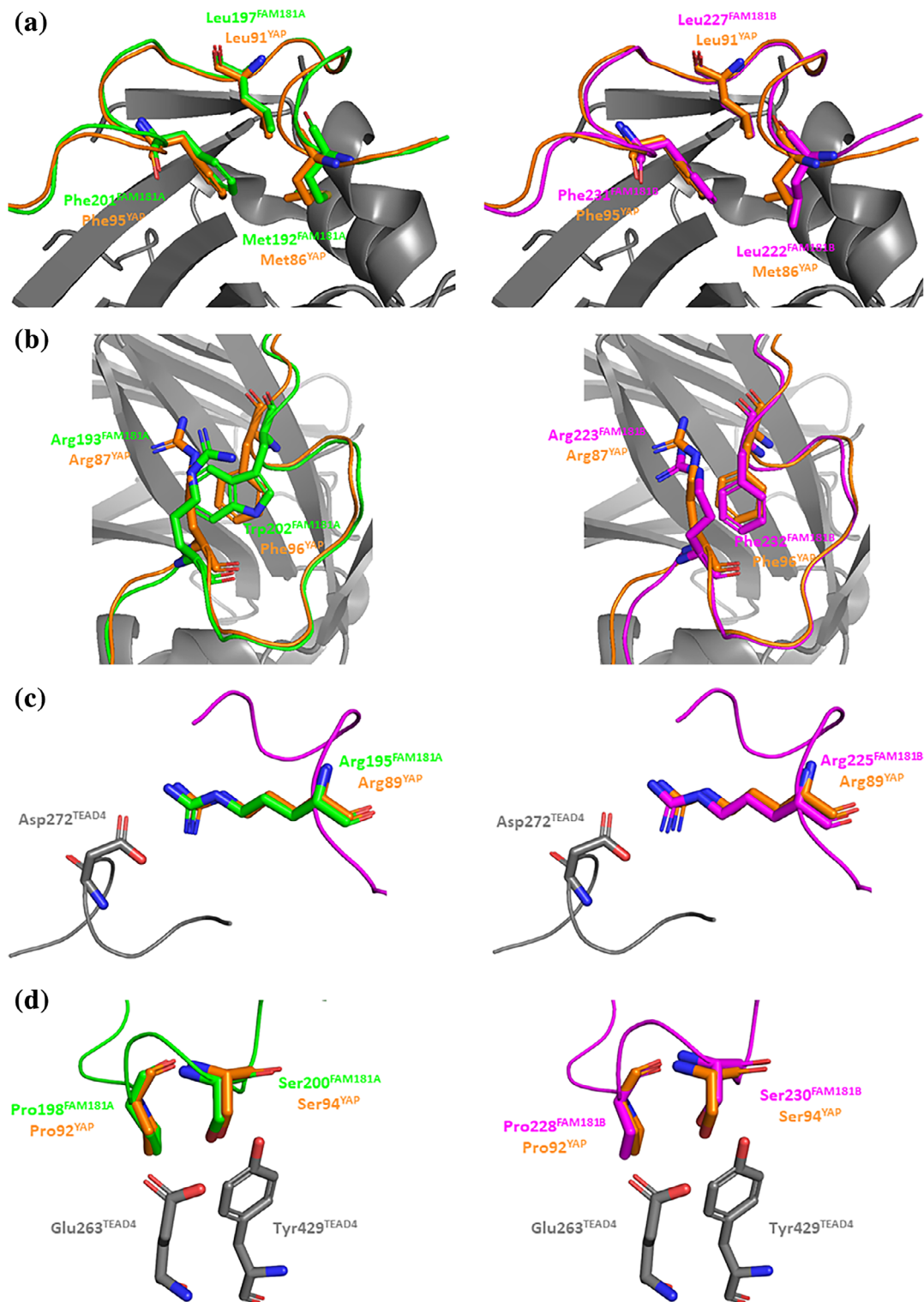


FIGURE 4 Key interactions between FAM181A^{190–205}/FAM181B^{220–235} and TEAD4. Left panels. The structures of the FAM181A^{190–205}:TEAD4 (pdb 6SEN) and YAP^{60–100}:TEAD4 (pdb 6GE3²⁶) complexes have been superimposed. The residues of FAM181A, YAP and TEAD are represented by green, orange and gray sticks, respectively. Right panels. The structures of the FAM181B^{220–235}:TEAD4 complexes (pdb 6SEO) and YAP^{60–100}:TEAD4 (pdb 6GE3²⁶) complexes have been superimposed. The residues of FAM181B, YAP and TEAD are represented by magenta, orange and gray sticks, respectively. (a). Hydrophobic core of the Ω -loop. (b). Residues involved in the stabilization of the hydrophobic core. (c). Salt bridge with Asp272^{TEAD4}. (d). Hydrogen bonds with Glu263^{TEAD4}:Tyr429^{TEAD4} and position of the conserved proline at the binding interface. The picture was drawn with PyMOL (Schrödinger Inc., Cambridge, Massachusetts)

(CD). In contrast to the CD spectrum obtained with TEAD4^{217–434}, which is characteristic of a well-folded protein (Figure S6a), the CD spectra of FAM181A^{127–205} and FAM181B^{157–237} show that—under our experimental conditions—these two fragments do not adopt a well-

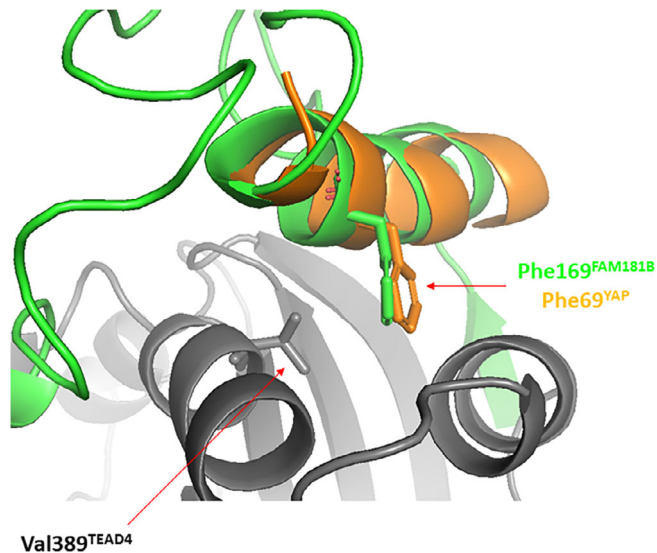


FIGURE 5 Interaction between the LxxLF motif and TEAD. A simulation of molecular dynamics was run using the FAM181B^{154–236}:TEAD^{217–434} complex (see text for details). The figure represents a superimposition between the conformation obtained after 10 ns simulation and the structure of the YAP:TEAD complex (PDB 3KYS¹⁶). FAM181B^{154–236} and TEAD^{217–434} and colored in green and gray, respectively. The YAP^{61–74} region from the YAP:TEAD structure is represented in orange. The picture was drawn with PyMOL (Schrödinger Inc., Cambridge, Massachusetts)

defined structure in solution. We also analyzed the amino acid sequence of full-length FAM181A/B with PrDOS (<http://prdos.hgc.jp>), a protein disorder prediction server.³³ This in silico analysis suggests that the regions corresponding to FAM181A^{127–205} and FAM181B^{157–237} are probably disordered in the context of the full-length proteins (Figure S6b).

Altogether, the data we obtained with FAM181A^{127–205} and FAM181B^{157–237} indicate that these two protein fragments are flexible both in solution and once bound to TEAD, suggesting that this high flexibility may have a negative contribution to their binding to TEAD.

2.5 | Study of the FAM181A/B:TEAD interaction in cells

The findings described above show that fragments of FAM181A/B and TEAD4 are able to interact and form stable complexes in a cell-free environment. To study this interaction in greater detail, we decided to investigate whether the full-length FAM181A/B and TEAD proteins can interact with each other in cells. To this end, N-terminally V5-tagged TEAD4 and (FLAG)₃-tagged FAM181A/B were co-transfected into HEK293FT cells. A V5-mediated immunoprecipitation of TEAD4 was performed and V5 and FLAG antibodies were used to detect TEAD4 and FAM181A/B, respectively, by Western blot. FAM181A and FAM181B are efficiently co-immunoprecipitated with wt^{TEAD4} (Figure 6). The FAM181A/B proteins were not detected in similar experiments carried out in the absence of V5-tagged TEAD4 (empty vector control), indicating that these proteins do not bind in a non-specific manner to the antibodies or beads

FIGURE 6 Interaction between FAM181A/B and TEAD4 in cells. N-terminally V5-tagged wtTEAD4 or Asp272Ala^{TEAD4} were co-transfected with (FLAG)₃-FAM181A/B into HEK293FT cells. TEAD4 was immunoprecipitated with a V5 specific antibody and co-immunoprecipitated FAM181A/B was determined by anti-FLAG Western blot. Left panel co-transfection FAM181A:TEAD4. Right panel co-transfection FAM181B:TEAD4. To provide a better view without signal saturation, a shorter exposure of total FAM181B is shown (flag in the lysates sub-panel). IP, Immunoprecipitated fraction

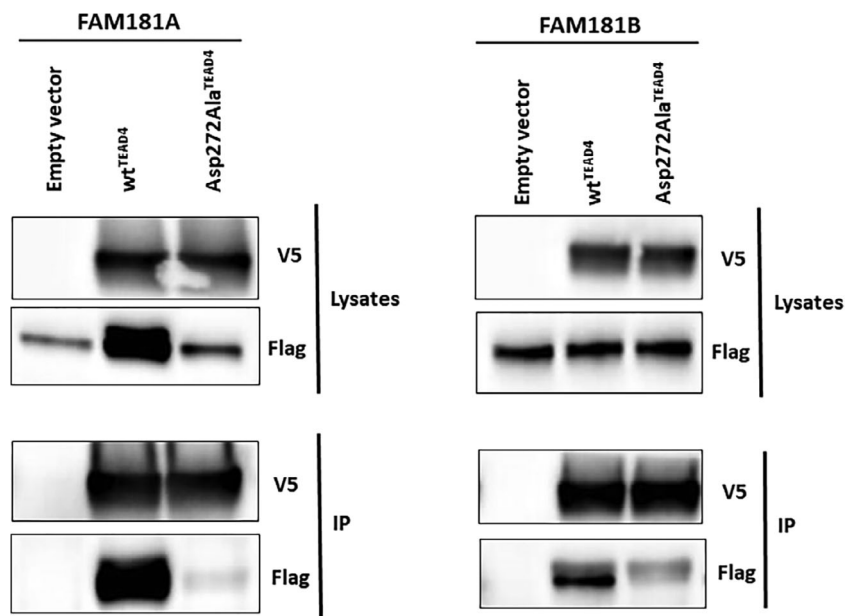


(Figure 6). To establish whether the observed interaction is specific, we used a mutated form of TEAD4, Asp272Ala^{TEAD4}. This mutation, which abolishes the formation of a salt bridge between Asp272^{TEAD4} and Arg195^{FAM181A}/Arg225^{FAM181B} (Figure 4c), reduces the affinity for TEAD4 of FAM181A^{127–205} ($K_d > 16 \mu\text{M}$, Figure S4) and FAM181B^{157–237} ($K_d > 75 \mu\text{M}$, Figure S4). The Asp272Ala^{TEAD4} mutation significantly affects the interaction between TEAD4 and FAM181A/B in co-immunoprecipitation experiments (Figure 6), showing that the observed interactions between the wild-type proteins are specific. Similar results were previously obtained with YAP, which interacts with Asp272^{TEAD4} via Arg89^{YAP} (Figure 4c).²⁸ We also repeatedly observed that the expression levels of FAM181A were significantly higher in co-transfection experiments performed with wt^{TEAD4} but not with Asp272Ala^{TEAD4} (Figure 6). Therefore, we quantified by ImageJ software (<https://imagej.nih.gov/ij/>) the IP over input ratio, normalized to the respective empty control within each experiment. Across three independent experiments, which exhibited a similar pattern, Asp272Ala^{TEAD4} consistently displayed an approximately fivefold reduction of co-IP capacity with FAM181A relative to wt^{TEAD4}. By similar quantification for FAM181B, Asp272Ala^{TEAD4} displayed an approximately fourfold reduction of co-IP capacity relative to wt^{TEAD4}. The observed effect of wt^{TEAD4} on the expression levels of FAM181A suggests that the formation of a complex between these two proteins may help enhancing the stability of FAM181A (at least in HEK293FT background and in conditions where this protein is overexpressed).

Overall, these data show that FAM181A/B and TEAD4 interact in a specific manner in the context of the full-length proteins in a cellular environment. This, together with the biochemical and structural data, supports the findings that FAM181A and FAM181B are TEAD interactors.

3 | DISCUSSION

The TEAD transcription factors bind to several proteins that modulate their activity. Currently, YAP, TAZ and VGLL1-4 are the best-characterized TEAD interactors. The TEAD-binding domain of YAP and TAZ is formed of a β -strand, an α -helix and an Ω -loop, while the current data show that the TEAD-binding domain of VGLL1-4 contains only a β -strand and an α -helix. In this article, we identify two new TEAD interactors, FAM181A and FAM181B. We show that a region of these two proteins adopts an Ω -loop conformation upon binding to TEAD and that the residues from this secondary structure element engage with TEAD interactions similar to those of

the corresponding residues from YAP. In a fashion similar to that of YAP, FAM181B also possesses an LxxLF motif (note that a VxxHF is present in VGLL1-4¹⁸). Site-directed mutagenesis experiments and molecular modeling studies suggest that the LxxLF motif of FAM181B and YAP bind to TEAD in a similar manner. FAM181A/B fragments containing only the Ω -loop or the Ω -loop plus the LxxLF motif (FAMB181B) have an affinity for TEAD in the low micromolar range. In transient transfection experiments, full-length FAM181A/B and TEAD interact with each other, and complex formation is prevented by a mutation that disrupts a key interaction at the Ω -loop binding pocket. Altogether, this indicates that FAM181A/B and TEAD can interact with each other both in biochemical assays and in a cellular environment.

The affinity for TEAD of the different FAM181A/B fragments that we have studied is lower than that of similar YAP, TAZ and VGLL1 constructs.^{31,34} This suggests that FAM181A/B may not easily gain access to TEAD in cells in the presence of these other proteins. However, the nuclear localization of TEAD regulators can be modulated by the Hippo pathway, and the phosphorylation of YAP, for example, leads to its sequestration in the cytoplasm.^{12,35} This suggests that, under specific physiological conditions, FAM181A/B may not need to compete with other TEAD regulators to form a complex with this transcription factor. Therefore, despite their lower affinity for TEAD, FAM181A/B proteins might be able to form transient complexes with this transcription factor *in vivo*.

Marks et al. have shown that the loss of FAM181B function did not lead to an obvious phenotype in mice, and they hypothesize that this lack of effect could be due to a possible redundancy between FAM181A and FAM181B.³⁰ This suggests that, to elucidate the biological relevance of the FAM181A/B:TEAD interaction, *in vivo* experiments will have to be conducted where the role of FAM181A and FAM181B is evaluated at the same time. While such studies are beyond the scope of this manuscript, our findings provide ideas on tools that could be used for such experiments. The analysis of the structure of the FAM181A/B:TEAD complexes suggest different mutations of FAM181A/B that can be designed to prevent the interaction with TEAD. For example, our data on the Asp272Ala^{TEAD4} mutation and earlier findings on the effect of the Arg89Ala^{YAP} mutation in cells¹⁶ suggest that Arg195Ala^{FAM181A} and Arg225Ala^{FAM181B} could be utilized as probes to determine the effect of the disruption of FAM181A/B:TEAD interactions in an *in vivo* set up. The cellular data obtained with Ser94Ala^{YAP16} also indicate that the Ser200Ala^{FAM181A}/Ser230Ala^{FAM181B} mutations could be used to disrupt the FAM181A/B:TEAD complex *in vivo*. Preliminary experiments we carried out in HEK293FT cells using a reporter gene under

the control of a YAP optimized promoter²⁸ did not show a modulation of TEAD transcriptional activity by FAM181A/B, suggesting that perhaps the conditions used to determine whether FAM181A/B exert an effect on TEAD transcriptional activity should be more physiological. For example, Honda et al. have utilized a luciferase gene under the control of a MYH7 promoter in C2C12 cells (mouse myoblasts) to study the effect of VGLL2 (selectively expressed in muscle cells) on TEAD.³⁶ Therefore, to determine the impact of FAM181A/B on TEAD transcriptional activity, reporter gene assays may have to be conducted in cells derived from a neural lineage using a reporter gene under the control of the promoter of a gene that is specifically expressed in that cell type. *Drosophila* has been an instrumental model organism for studying the role of the Hippo pathway in development, and it is a very attractive system for studying the *FAM181A/B* genes. Unfortunately, our motif search only identified Yorkie, the drosophila homolog of YAP, but not FAM181A/B, suggesting that these proteins are not present in flies (Appendix S1).

In summary, the discovery of FAM181A/B as new TEAD interactors paves the way for future in vivo studies to elucidate the relevance of this interaction in the context of the development of the nervous system and to gain better knowledge on the physiological role of the FAM181A/B:TEAD complex.

4 | MATERIAL AND METHODS

4.1 | Database search

The Motif Search algorithm from GenomeNet (www.genome.jp) was used to interrogate the GenBank, UniProt, RefSeq and PDBSTR databases. Three operators were utilized to create degenerate sequence motifs: x represents any amino acid; [AB] means either amino acid A or B; {A} means any amino acid except A. The amino acid sequence of human YAP corresponding to residues 85–99, which adopts an Ω -loop conformation upon binding to TEAD, was used as template sequence for the database search. Structural data and results from structure–function studies were combined to identify the residues from YAP^{85–99} which do not interact with TEAD in the YAP:TEAD complex (e.g., residues with the side chain pointing to the solvent).^{15,16,20,25–28} On the basis of this initial analysis, several positions were annotated with x (85-P-x-R-x-R-x-L-P-x-S-F-F-x-x-P-99) indicating that any amino acid can occupy them. The first search was used to determine whether amino acids other than a serine could be present at position-94 (Motif_01, Figure S1). The sequences obtained were individually analyzed using the

structural data to determine whether the amino acids identified at position-94 could engage in favorable interactions with TEAD. All the sequences identified contained a glutamate residue at position-94. According to the structure of the YAP:TEAD complex, such residues should not be tolerated at the binding interface, because this would result in a steric clash with Tyr429^{TEAD4} and repulsive electrostatic interactions with Glu263^{TEAD4}.²⁶ On the basis of this result, a serine was maintained at position-94 and a search with Motif_02 was conducted (Figure S1). This methodology was repeated with a total of 14 motifs to obtain the final consensus sequence: P-x-[RKHS]-x-R-x-[LMF]-P-x-S-F-[FW]-x-x-P. The databases were interrogated with this motif to generate the list of the sequences used in this communication (Appendix S2).

4.2 | Peptides

The synthetic peptides (both N-acetylated and C-amidated) were purchased from Biosynthan (Germany). The purity (>90%) and the chemical integrity of the peptides was determined by liquid chromatography–mass spectrometry (LC–MS) from 10 mM stock solutions in 90:10 (v/v) dimethyl sulfoxide (DMSO):water.

4.3 | Proteins

The amino acid sequences of full length FAM181A (UniProt Q8N9Y4) and FAM181B (UniProt A6NEQ2) were back-translated into an *Escherichia coli* codon-optimized DNA sequence by an in-house tool and synthesized by GeneArt (Thermo Fisher Scientific, Germany). The DNA fragment encoding FAM181A^{127–205} was PCR-amplified with primers comprising LguI restriction sites and cloned into a pET-derived vector with an N-terminal His₆-Gly-Ser spacer-Lipoyl-Gly-Ser spacer-HRV3C affinity purification and solubilizing tag.³⁷ The DNA fragment encoding FAM181B^{159–237} was PCR-amplified with primers comprising LguI restriction sites for seamless cloning into a pET-derived vector with an N-terminal His₆-Gly-Ser spacer-Rbx-Gly-Ser spacer-HRV3C affinity purification and solubilizing tag.³⁸ The FAM181B fragment in the resulting expression plasmid was N-terminally extended by adding residues 157 and 158 through site-directed mutagenesis with the QuikChange II Lightning Site-Directed Mutagenesis kit (Agilent, Santa Clara, California). The DNA sequence of all expression constructs was verified by Sanger sequencing. Recombinant FAM181A^{127–205} and FAM181B^{157–237} proteins were purified using identical protocols. The

expression plasmid was transformed into NiCo21 (DE3) competent *E. coli* cells (New England Biolabs, Ipswich, Massachusetts). TB medium supplemented with 50 mM MOPS was inoculated with a bacterial pre-culture and incubated under constant shaking at 37°C. At OD₆₀₀ = 0.8, the culture was chilled to 18°C, and protein expression was induced by addition of 0.2 mM Isopropyl β-D-1-thiogalactopyranoside. After overnight expression, the bacteria were harvested by centrifugation for 20 min at 6,000g, frozen on dry ice and stored at -80°C. The cell pellets were thawed and suspended in buffer A (50 mM Tris-HCl, 300 mM NaCl, 30 mM imidazole, pH 8.0) supplemented with cOmplete protease inhibitor (Roche, Switzerland) and TurboNuclease (Merck, Germany). The cells were mechanically disrupted by three passages through an EmulsiFlex C3 homogenizer (Avestin, Canada), and insoluble cell debris was removed by centrifugation for 30 min at 40,000g. The clarified cell lysate was loaded onto two 1 ml HisTrap HP columns (GE Healthcare, UK) mounted in series on an ÄKTA Pure chromatography system (GE Healthcare). Contaminating proteins were washed away with 10 column volumes of buffer A, and the His-tagged protein was eluted with a linear gradient over 10 column volumes to 100% buffer B (buffer A with 300 mM imidazole). The N-terminal purification tag was cleaved off overnight at 5°C by His₆-tagged HRV 3C protease during dialysis against buffer A. The cleaved protein was passed over the re-equilibrated HisTrap HP columns to remove the cleaved tag, HRV3C-protease, and contaminating host cell proteins. The fractions containing the FAM181A/B proteins were pooled, concentrated with Amicon Ultra-15 3 K centrifugal filter unit (Merck, Germany) and loaded onto a HiLoad Superdex 75 16/600 pg size exclusion column (GE Healthcare, United Kingdom) equilibrated with 50 mM Tris-HCl, 150 mM NaCl, 10% glycerol, pH 8.0. The fractions containing pure protein were pooled and concentrated to about 2 mg/ml in an Amicon filter unit (Merck, Germany). Purity and concentration of the protein samples were determined by RP-UHPLC, measuring the absorbance at 210 nm. The concentration was calculated using a BSA standard curve as reference. Identity and molecular weight of the FAM181A/B proteins were confirmed by LC-MS. The final yield was about 10 mg/L expression culture. The different TEAD4 variants were purified as previously described.²⁸

4.4 | Time-resolved FRET, surface Plasmon resonance and circular dichroism

Biotinylated N-Avitagged-TEAD4²¹⁷⁻⁴³⁴ (1 nM; wt^{TEAD4}) and LANCE Eu-W1024 Streptavidin (0.5 nM, PerkinElmer,

Waltham, Massachusetts) were pre-incubated for 1 hr at room temperature in 50 mM HEPES pH 7.4, 100 mM KCl, 0.05% (v/v) Tween-20, 0.25 mM TCEP, 1 mM, and 0.05% (w/v) BSA. N-terminally Cy5-labelled YAP⁶⁰⁻¹⁰⁰ (20 nM) and serial dilutions of the peptides/protein fragments to be tested were added and incubated in white 384-well plates (Greiner Bio-One International, Austria) for 1 hr at room temperature. DMSO was present at 2% in the assay. The solubility of the peptides in assay buffer was measured by dynamic light scattering with a Dyna Prot device (Wyatt technology Corp., Germany). The fluorescence in the TR-FRET assay was measured with a Genios Pro reader (Tecan, Switzerland) (50 μs delay between excitation and fluorescence, 75 μs integration time, excitation wavelength 340 nm, emission wavelengths 620 and 665 nm). Data analyses were carried out using the TR-FRET 665/620 nm emission ratio. The IC₅₀ values were obtained by nonlinear regression analysis with GraphPad Prism (GraphPad Software, San Diego, California). The Surface Plasmon Resonance and Circular Dichroism experiments were conducted as previously described.²⁸

4.5 | Structural biology

The untagged wtTEAD4²¹⁷⁻⁴³⁴ protein used for crystallization was obtained as described previously.²⁵ Complex crystals between myristoylated wtTEAD4²¹⁷⁻⁴³⁴ and the FAM181 peptides were grown at 293 K using the sitting drop vapor diffusion method. wtTEAD4²¹⁷⁻⁴³⁴ (7.4 mg/ml) and FAM181A¹⁹⁰⁻²⁰⁵ or FAM181B²²⁰⁻²³⁵ (0.5 mM) were pre-incubated in 25 mM Tris-HCl pH 8.0, 100 mM NaCl and 1 mM TCEP (molar ratio peptide:protein = 1.7). For crystallization, the FAM181A/B:TEAD4 complexes were mixed with an equal volume of reservoir solution (0.3 + 0.3 μl). Reservoir solutions: FAM181A¹⁹⁰⁻²⁰⁵:TEAD4 complex—200 mM (NH₄)₂SO₄, 100 mM CH₃COONa(H₂O)₃ pH 4.59 and 35% pentaerythritol ethoxylate (15/4 EO/OH); FAM181B²²⁰⁻²³⁵:TEAD4 complex—50 mM (NH₄)₂SO₄, 50 mM Bis-Tris pH 6.5 and 30% pentaerythritol ethoxylate (15/4 EO/OH). For data collection, the FAM181A¹⁹⁰⁻²⁰⁵:TEAD4 crystals were directly shock-cooled in liquid nitrogen while the FAM181B²²⁰⁻²³⁵:TEAD4 crystals were first soaked for a few seconds in the reservoir solution containing 30% glycerol before shock-cooling in liquid nitrogen. X-ray diffraction data were collected at the Swiss Light Source (SLS, beamline X10SA) using a Pilatus pixel detector. Raw diffraction data were analyzed and processed using the autoPROC³⁹/STARANISO (Global Phasing Ltd., UK) toolbox. The structures were solved by molecular replacement with PHASER⁴⁰ using as search model the coordinates of previously solved in-house structures of TEAD4.

The software COOT⁴¹ and BUSTER (Global Phasing Ltd.) were used for iterative rounds of model building and structure refinement. The refined coordinates of the complex structures have been deposited in the Protein Data Bank ([www.wwpdb.org](http://www wwpdb.org)) with the accession numbers 6SEN (FAM181A^{190–205}:TEAD4) and 6SEO (FAM181B^{220–235}:TEAD4).

4.6 | Cellular biology

Cloning. nV5-tagged TEAD4 cDNA constructs (wt^{TEAD4} and Asp272Ala^{TEAD4}) were described previously.²⁸ FAM181A (RefSeq NM_138344.5) was amplified by standard PCR from a pDONR221-FAM181A (human codon-optimized) clone, obtained from GeneArt (Thermo Fisher Scientific, Germany), using primers containing N-terminal (FLAG)₃ epitope. The PCR product was cloned by Gateway reaction into pcDNA3.1 Hygro-DEST (Invitrogen, Carlsbad, California), according to the manufacturer's protocol. FAM181B (RefSeq NM_17885.4) was amplified by standard PCR from a pcDNA-DEST40-FAM181B (human codon-optimized) clone using primers containing N-terminal (FLAG)₃ epitope. The PCR product was cloned by Gateway reaction into pcDNA3.1 Hygro-DEST (Invitrogen), according to the manufacturer's protocol.

Cell culture and transfections. HEK293FT cells, cell culture handling and Lipofectamine 2000-based transient transfections were described previously.²⁸

TEAD/FAM181 co-immunoprecipitation (co-IP). For FAM181A co-IP experiments, HEK293FT cells were transfected with nV5-TEAD4 and (FLAG)₃-FAM181B constructs (1:1 ratio), and lysed in NP40 buffer (Invitrogen) containing PhosSTOP and Protease Inhibitor Cocktail (both from Roche, Switzerland) 48 hr after transfection. For FAM181B co-IP experiments, HEK293FT cells were transfected with nV5-TEAD4 and (FLAG)₃-FAM181B constructs (1.5:1 ratio), and the proteins were extracted from nuclei using the NE-PERTM Nuclear (Thermo Fisher Scientific, Germany) 48 hr after transfection. Lysates (100 µg) were then incubated with V5 antibody overnight (FAM181B co-IP) or for 2 hr (FAM181A co-IP) under rotation at 4°C, followed by incubation with Dynabeads Protein G (Invitrogen) for 2 hr under rotation at 4°C. Immunoprecipitates were washed three times with NP40 buffer containing protease and phosphatase inhibitors, eluted with Laemmli Sample Buffer (BioRad, Hercules, California) by incubation at 95°C for 5 min and resolved by standard SDS-PAGE gel electrophoresis and Western blotting. Antibodies for IP: V5 (Invitrogen). Antibodies for Western blot: FLAG (Sigma-Aldrich, St. Louis, Michigan) and V5 (Cell Signaling Technology, Danvers, Massachusetts) as primary

antibodies; HRP-anti-rabbit (Cell Signaling Technology) as secondary antibody.

The TEAD transcription factors are regulated by different proteins. Combining structural data and motif searches in protein databases FAM181A and FAM181B were identified as new TEAD interactors. Biochemical and structural data reveal that FAM181A/B bind to TEAD via an Ω-loop and this interaction was also demonstrated in a cellular context. The FAM181A/B:TEAD interaction might play a role in the development of the nervous system as FAM181A/B are specifically expressed in this tissue.

ACKNOWLEDGMENTS

The authors thank Aude Izaac, Suzanne Chau, Aurélie Winterhalter, Patrick Graff and René Hemmig for excellent technical assistance. X-ray data collection was performed on the X10SA beamline at the Swiss Light Source, Paul Scherrer Institute, Villigen, Switzerland.

CONFLICT OF INTEREST

The authors declare no conflict of interest.

ORCID

Patrick Chène  <https://orcid.org/0000-0002-6010-9169>

REFERENCES

1. Wang Y, Yu A, Yu FX. The hippo pathway in tissue homeostasis and regeneration. *Protein Cell*. 2017;8:349–359.
2. Santucci M, Vignudelli T, Ferrari S, et al. The hippo pathway and YAP/TAZ-TEAD protein-protein interaction as targets for regenerative medicine and cancer treatment. *J Med Chem*. 2015;58:4857–4873.
3. Zhang K, Qi HX, Hu ZM, et al. YAP and TAZ take center stage in cancer. *Biochemistry*. 2015;54:6555–6566.
4. Zanconato F, Cordenonsi M, Piccolo S. YAP/TAZ at the roots of cancer. *Cancer Cell*. 2016;29:783–803.
5. Holden JK, Cunningham CN. Targeting the hippo pathway and cancer through the TEAD family transcription factors. *Cancer*. 2018;10:E81.
6. Moya IM, Halder G. Hippo-YAP/TAZ signalling in organ regeneration and regenerative medicine. *Nat Rev Mol Cell Biol*. 2018;20:211–226.
7. Wang J, Liu S, Heallen T, Martin JF. The hippo pathway in the heart: Pivotal roles in development, disease, and regeneration. *Nat Rev Cardiol*. 2018;15:672–684.
8. Landin-Malt A, Benhaddou A, Zider A, Flagiello D. An evolutionary, structural and functional overview of the mammalian TEAD1 and TEAD2 transcription factors. *Gene*. 2016;591:292–303.
9. Lin KC, Park HW, Guan KL. Regulation of the hippo pathway transcription factor TEAD. *Trends Biochem Sci*. 2017;42:862–872.
10. Hilman D, Gat U. The evolutionary history of YAP and the hippo/YAP pathway. *Mol Biol Evol*. 2011;28:2403–2417.
11. Simon E, Fauchoux C, Zider A, Thézé N, Thiébaud P. From vestigial to vestigial-like: The *Drosophila* gene that has taken wing. *Dev Genes Evol*. 2016;226:297–315.

12. Callus BA, Finch-Edmondson ML, Fletcher S, Wilton SD. YAPing about and not forgetting TAZ. *FEBS Lett.* 2019;593:253–276.
13. Jacquemin P, Sapin V, Alsat E, Evain-Brion D, Dollé P, Davidson I. Differential expression of the TEF family of transcription factors in the murine placenta and during differentiation of primary trophoblasts *in vitro*. *Dev Dyn.* 1998;212:423–436.
14. Fossdal R, Jonasson F, Kristjansdottir GT, et al. A novel TEAD1 mutation is the causative allele in Sveinsson's chorioretinal atrophy (helicoid peripapillary chorioretinal degeneration). *Hum Mol Genet.* 2004;13:975–981.
15. Chen L, Chan SW, Zhang XQ, et al. Structural basis of YAP recognition by TEAD4 in the hippo pathway. *Genes Dev.* 2010;24:290–300.
16. Li Z, Zhao B, Wang P, et al. Structural insights into the YAP and TEAD complex. *Genes Dev.* 2010;24:235–240.
17. Kaan HYK, Chan SW, Tan SKJ, et al. Crystal structure of TAZ-TEAD complex reveals a distinct interaction mode from that of YAP-TEAD complex. *Sci Rep.* 2017;7:2035.
18. Pobbati AV, Chan SW, Lee I, Song H, Hong W. Structural and functional similarity between Vgll1-TEAD and YAP-TEAD complexes. *Structure.* 2012;20:1135–1140.
19. Jiao S, Wang H, Shi Z, et al. A peptide mimicking VGLL4 function acts as a YAP antagonist therapy against gastric cancer. *Cancer Cell.* 2014;25:166–180.
20. Bokhovchuk F, Mesrouze Y, Izaac A, et al. Molecular and structural characterization of a TEAD mutation at the origin of Sveinsson's chorioretinal atrophy. *FEBS J.* 2019;286:2381–2398.
21. Belandia B, Parker MG. Functional interaction between the p160 coactivator proteins and the transcriptional enhancer factor family of transcription factors. *J Biol Chem.* 2000;275:30801–30805.
22. Leszczynski JF, Rose GD. Loops in globular proteins: A novel category of secondary structure. *Science.* 1986;234:849–855.
23. Ring CS, Kneller DG, Langridge R, Cohen FE. Taxonomy and conformational analysis of loops in proteins. *J Mol Biol.* 1992;224:685–699.
24. Fetrow JS. Omega loops: Nonregular secondary structures significant in protein function and stability. *FASEB J.* 1995;9:708–717.
25. Mesrouze Y, Meyerhofer M, Bokhovchuk F, et al. Effect of the acylation of TEAD4 on its interaction with co-activators YAP and TAZ. *Protein Sci.* 2017;26:2399–2409.
26. Mesrouze Y, Bokhovchuk F, Izaac A, et al. Adaptation of the bound intrinsically disordered protein YAP to mutations at the YAP:TEAD interface. *Protein Sci.* 2018;27:1810–1820.
27. Zhang Z, Lin Z, Zhou Z, et al. Structure-based design and synthesis of potent cyclic peptides inhibiting the YAP-TEAD protein-protein interaction. *ACS Med Chem Lett.* 2014;5:993–998.
28. Mesrouze Y, Bokhovchuk F, Meyerhofer M, et al. Dissection of the interaction between the intrinsically disordered YAP protein and the transcription factor TEAD. *Elife.* 2017;6:e25068.
29. Chen L, Loh PG, Song H. Structural and functional insights into the TEAD-YAP complex in the hippo signaling pathway. *Protein Cell.* 2010;1:1073–1083.
30. Marks M, Pennimpede T, Lange L, Grote P, Herrmann BG, Wittler L. Analysis of the *Fam181* gene family during mouse development reveals distinct strain-specific expression patterns, suggesting a role in nervous system development and function. *Cancer.* 2016;575:438–451.
31. Hau JC, Erdmann D, Mesrouze Y, et al. The TEAD4-YAP/TAZ protein-protein interaction: Expected similarities and unexpected differences. *Chembiochem.* 2013;14:1218–1225.
32. Mesrouze Y, Erdmann D, Zimmermann C, Fontana P, Schmelzle T, Chène P. Different recognition of TEAD transcription factor by the conserved β -strand:Loop: α -helix motif of the TEAD-binding site of YAP and VGLL1. *ChemistrySelect.* 2016;1:2993–2997.
33. Ishida T, Kinoshita K. PrDOS: Prediction of disordered protein regions from amino acid sequence. *Nucleic Acids Res.* 2007;35:W460–W464.
34. Mesrouze Y, Hau JC, Erdmann D, et al. The surprising features of the TEAD4-Vgll1 protein-protein interaction. *Chembiochem.* 2014;15:537–542.
35. Shreberk-Shadek M, Oren M. New insights into YAP/TAZ nucleo-cytoplasmic shuttling: New cancer therapeutic opportunities? *Mol Oncology.* 2019;13:1335–1341.
36. Honda M, Tsuchimochi H, Hitachi K, Ohno S. Transcriptional cofactor Vgll2 is required for functional adaptations of skeletal muscle induced by chronic overload. *J Cell Physiol.* 2019;234:15809–15824.
37. Lebendiker M, Danieli T. Production of prone-to-aggregate proteins. *FEBS Lett.* 2014;588:236–246.
38. Kohli BM, Ostermeier C. A Rubredoxin based system for screening of protein expression conditions and on-line monitoring of the purification process. *Protein Expr Purif.* 2003;28:362–367.
39. Vonrhein C, Flensburg C, Keller P, et al. Data processing and analysis with the autoPROC toolbox. *Acta Cryst D.* 2011;67:293–302.
40. McCoy AJ, Grosse-Kunstleve RW, Adams PD, Winn MD, Storoni LC, Read RJ. PHASER crystallographic software. *J Appl Cryst.* 2007;40:658–674.
41. Emsley P, Cowtan K. Coot: Model-building tools for molecular graphics. *Acta Crystallogr.* 2004;D60:2126–2132.

SUPPORTING INFORMATION

Additional supporting information may be found online in the Supporting Information section at the end of this article.

How to cite this article: Bokhovchuk F, Mesrouze Y, Delaunay C, et al. Identification of FAM181A and FAM181B as new interactors with the TEAD transcription factors. *Protein Science.* 2020;29:509–520. <https://doi.org/10.1002/pro.3775>